

Coupled thermomechanics of single-wall carbon nanotubes

F. Scarpa,^{1,a)} L. Boldrin,¹ H. X. Peng,¹ C. D. L. Remillat,¹ and S. Adhikari²

¹Advanced Composites Centre for Innovation and Science, Aerospace Engineering, University of Bristol, BS8 1TR Bristol, United Kingdom

²Multidisciplinary Nanotechnology Centre, University of Swansea, SA2 8PP Swansea, United Kingdom

(Received 9 August 2010; accepted 27 August 2010; published online 11 October 2010)

The temperature-dependent transverse mechanical properties of single-walled nanotubes are studied using a molecular mechanics approach. The stretching and bond angle force constants describing the mechanical behavior of the sp^2 bonds are resolved in the temperature range between 0 and 1600 K, allowing to identify a temperature dependence of the nanotubes wall thickness. We observe a decrease of the stiffness properties (axial and shear Young's modulus) with increasing temperatures, and an augmentation of the transverse Poisson's ratio, with magnitudes depending on the chirality of the nanotube. Our closed-form predictions compare well with existing molecular dynamics simulations. © 2010 American Institute of Physics. [doi:10.1063/1.3499748]

The behavior of carbon nanotubes (CNTs) and its composites^{1,2} has generated a wealth of activities to identify their thermal conductivity,^{3–7} Young's modulus and tensile strength [simulated with molecular dynamics (MD) and atomistic-FE],^{8–13} and stiffness at different temperatures. The use of simulations to predict the thermal dependence of the nanotubes mechanical properties is a necessity, because of the difficulties to obtain direct experimental measurements in different thermal environments. However, all the predictive tools so far available to simulate and design the stiffness of CNT-based composites are not based on analytical formulas that would facilitate the work of the material scientist and engineer. The existing atomistic-continuum models for the elastic properties of CNTs in closed form^{14,15} have their bonds force constants formulated only for room temperature. In this work we propose the results from a compact formulation that express the relation between the sp^2 C–C bond force constants and the surrounding temperature of the nanotube, providing a functional description of the coupled thermal and mechanical linear elastic properties of SWCNTs.

Our model is based on the universal force field (UFF) formulation, where the harmonic potential energies associated to stretching, bending and out-of-plane torsion are linked to correspondent force constants $k_{IJ}^T, k_{JK}^T, K_{IJKL}$, respectively.¹⁶ Details of the development of the model are illustrated in the Supplementary Material. The stretching, bending and torsional force constants are a function of the equilibrium lengths between bonds IJ and JK . While the torsional constant shows an extremely low sensitivity with temperature, the other force constants are linked to the thermal environment through the relation $r_{IJ} = r_{JK} = r_{IJ}^0(1 + \alpha\Delta T)$,¹³ where $r_{IJ}^0 = 0.142$ nm and α is the coefficient of thermal expansion (CTE). In this work, we consider as CTE for the bond the one identified in suspended graphene sheets using a nonuniform Green's function approach by Jiang *et al.*¹⁷ The equivalent mechanical behavior of the C–C bond is represented at this stage by equating the harmonic potentials with the correspondent strain energies deformations under axial, bending and torsion of a structural beam element with deep shear deformation and circular cross section.¹⁸ The mechani-

cal behavior of the beams is provided by the equivalent materials and geometry properties of the bond (Young's modulus E , Poisson's ratio ν , and thickness d). The equivalence of the harmonic potentials and the strain energies, together with the assumption of isotropic equivalent material properties of the bonds, leads to a system of nonlinear equations that yields a unique value of the thickness d for a given temperature T .

At room temperature, the thickness identified using this approach yields a value of 0.084 nm, equal to the one found for single wall and nanotube bundles in Ref. 19. We observe a low sensitivity of the thickness corresponding to the isotropic condition versus the temperature, with a minimum value of 0.0835 nm at 1600 K, and a maximum value of 0.0841 nm for $T=470$ K. It is interesting to notice that the C–C bond behaves mechanically as if made of a quasizero Poisson's ratio behavior, like in natural-occurring cork.²⁰ The 0.084 nm value at room temperature is also consistent with the 0.084 nm found by Kudin *et al.*, and 0.074 nm identified by Tu and Ou-Yang.²¹ Batra and Sears have found equivalent thickness values ranging between 0.043²² and 0.1 nm.²¹ Zhang and Shen identify thickness of 0.088 nm and 0.087 nm for (17,0) and (21,0) nanotubes, respectively, while for (10,10) and (12,12) the thickness calculated is 0.067 nm.¹⁰ The thickness values calculated with our method do compare well with the 0.080 nm of Chen and Cao, although they are higher than the 0.066 nm of Yakobson *et al.*, and 0.60 nm of Vodenitcharova and Zhang.²¹

Classical mechanistic theories for the elastic properties of single-wall carbon nanotubes consider the strain energy associated to the deformation of sp^2 bonds in terms of global stretching and bond angle constants (C_ρ and C_θ , respectively^{14,15}). For the bond angle constant (moment), we consider that for linear elasticity the lattice is dominated by hinging deformation,²³ and determine the hinging constant accordingly (Fig. 1). For room temperature we obtain a value of 1.44 nN nm rad⁻², well in line with the 1.42 nN nm rad⁻² used in Refs. 14 and 15. The stretching constant is calculated as $C_\rho = k_\rho k_{IJ}^T$, where $k_\rho = 1.128$ is used to converge to the 0.36 T Pa nm⁻¹ of the in-plane graphitic surface modulus (chiral index $n \rightarrow \infty$).²³ At room temperature, we identify a stretching constant equal to 735 nN nm⁻¹, which compares

^{a)}Electronic mail: f.scarpa@bristol.ac.uk.

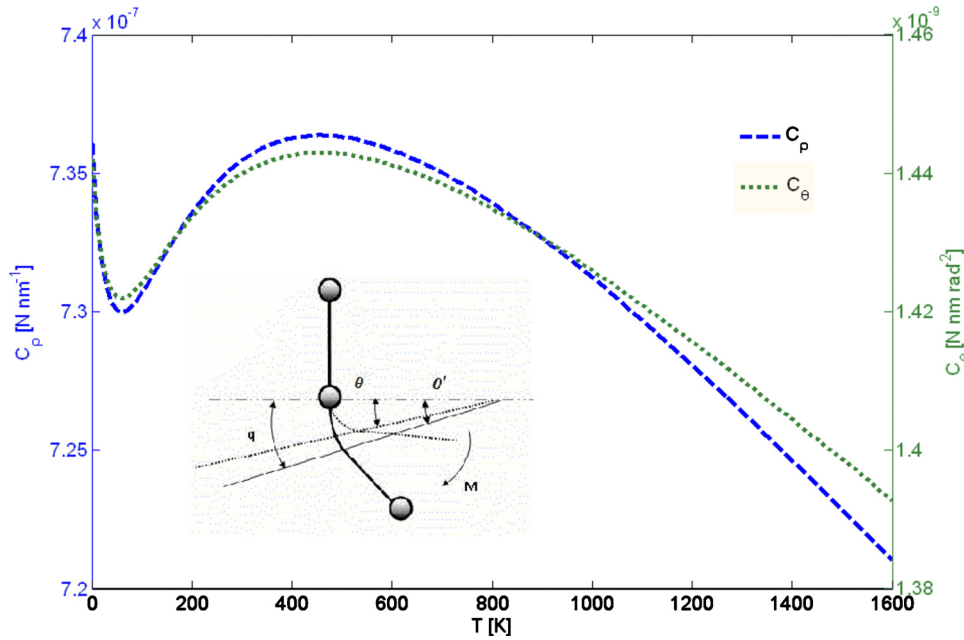


FIG. 1. (Color online) The variation in the stretching constant C_p and hinging constant C_θ over the temperature. The hinging constant is calculated from the change in angular deformation $\theta - \theta' = \Delta\theta = \int_0^q \frac{M}{EI} dq = Mq/EI$. Under hinging, only the initial portion $q = r_{IJ}/5$ of the bond length deforms by rotation, while the rest deforms as a rigid body (Ref. 24). The hinging constant is then defined as $C_\theta = M/\Delta\theta = EI/q = k_{IJ}^T d^2 r_{IJ}/16$.

well with the 742 nN nm^{-1} used by Shen and Li.¹⁵ Cadelano *et al.*²⁵ identify the surface modulus of graphene-type systems equal to $0.312 \text{ T Pa nm}^{-1}$ at zero temperature damped dynamics, 6% lower than our result ($0.332 \text{ T Pa nm}^{-1}$). For both bending and stretching constants, we observe a very low dependence versus temperature between $370 \text{ K} < T < 570 \text{ K}$. The stretching constant then decreases with increasing temperatures with an approximate rate of $0.015 \text{ nN nm}^{-1} \text{ K}^{-1}$, a behavior similar to the one of the C_θ constant, having the latter a decrease rate of $4.910^{-5} \text{ nN nm rad}^{-2} \text{ K}^{-1}$ between 600 and 1600 K. At low temperatures, both the force and bending constants decrease from values equal to 99.2% of the maximum C_θ and C_p at 1 K to a minimum at 70 K corresponding to the 98.6% of the maximum of the constants at 450 K. Similarly to the C–C bond thickness, the force stretching and bending constants can be expressed in polynomial terms (see Ref. 26).

To simulate the coupled thermomechanics of SWCNTs (axial and shear stiffness, and Poisson's ratio), we use the constants C_p and C_θ within the formulation proposed by Shen and Li.¹⁵ We compare the surface Young's modulus Y_{11}^s calculated in analytical form against the results obtained through MD simulations using a REBO potential by Zhang and Shen¹⁰ (Fig. 2).

In terms of longitudinal modulus Y_{11}^l (defined as Y_{11}^s/d), our simulations tend to overestimate the MD results from,¹⁰ with our axial moduli for (17,0) nanotubes being 9% higher than the molecular dynamics simulations at $T=300 \text{ K}$, while at a temperature of 1000 K our overestimate is around 11%. Our predictions are also well in line with the $0.352 \text{ T Pa nm}^{-1}$ of Tu and Ou-Yang and Pantano *et al.*²¹ although 3.5% higher than Li and Chou and Wang and co-authors.²⁷ The effective Young's modulus $Y_{11} = Y_{11}^s/(R/2)$ (where R is the diameter of the nanotube) has been also derived by Hsieh *et al.*¹¹ (Fig. 3), showing a general agreement between trends related to the nanotube radius at $T=1100 \text{ K}$, and within the temperature range 50–1100 K.

We observe also an overestimate for the shear modulus G_{12} ,¹⁰ with discrepancies around 29% and 28% at 1000 K and 1200 K, respectively. However, our predictions show a

decrease in the longitudinal shear modulus versus the temperature, opposite from the results derived in Ref. 10.

The transverse Poisson's ratio ν_{21} increases with the temperature (Fig. 4), although the augmentation is limited on average to a 3% increase between $T=300 \text{ K}$ and 1200 for the different chirality and tube diameters. The low sensitivity of the Poisson's ratio over the temperature is due to the weak dependency versus the temperature itself of the term $C_p r_{IJ}^2/C_\theta$, which is contained both in the numerator and denominator of the Poisson's ratio expression.¹⁵ Chen *et al.*¹³ observe also an increase in ν_{21} with temperature (31% of increase for zigzag tubes of 1.2 nm diameter between room temperature and $T=1200 \text{ K}$), due mainly to the use in their model of a CTE positive for $T > 298 \text{ K}$, while in our approach we have $\text{CTE} > 0$ for 650 K.¹⁷ Zhang and Shen predict a transverse Poisson's ratio for a (17,0) nanotube at $T=300 \text{ K}$ equal to 0.17, in good agreement with our value of 0.16.¹⁰ For graphene-type systems, our model predicts at zero temperature a Poisson's ratio of 0.12, significantly lower than the 0.31 identified in Ref. 25. However, our range

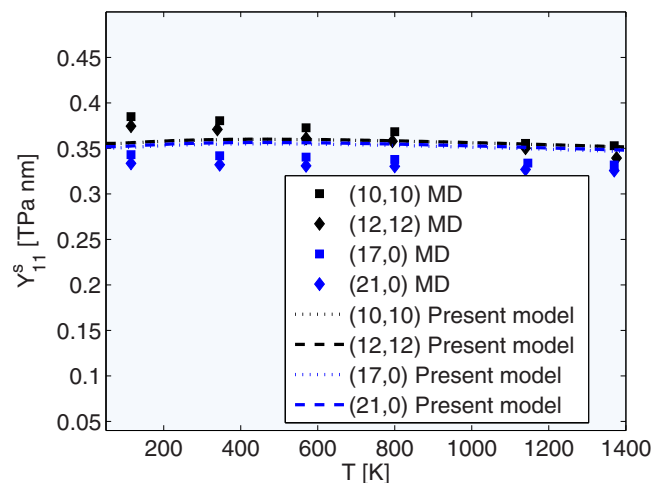


FIG. 2. (Color online) SWCNT surface Young's modulus against MD simulations from Ref. 10.

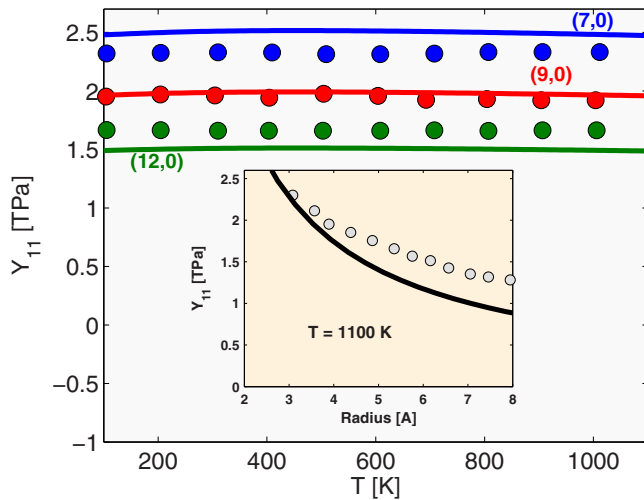


FIG. 3. (Color online) Comparison of the effective Young's modulus for $(n,0)$ SWCNTs against values from Ref. 11 (circular dots).

of Poisson's ratios at room temperature for zigzag tubes (Fig. 4) is in line with the 0.12–0.19 values predicted by Sanchez-Portal *et al.*, the 0.15 of Kudin and co-authors, 0.21 of Sears and Batra, and 0.24 from Zhou *et al.*²¹

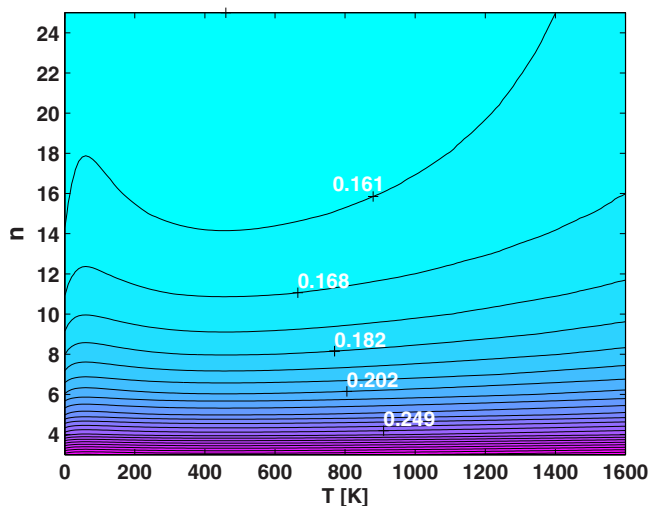


FIG. 4. (Color online) Map of the transverse Poisson's ratio ν_{21} for $(n,0)$ tubes vs the chiral index n and temperature.

In summary, our model allows to predict in a compact form the overall elastic transverse properties of single wall nanotubes over a large temperature range. The bending and stretching constants identified with our approach capture the intrinsic hinging/stretching behavior of sp^2 C–C bonds in nanotubes, and relate the stiffness and Poisson's ratio to the ambient temperature of the nanotube, with 2% average decrease in the Young's modulus between the ambient temperature and 1200 K for a given tube chirality.

- ¹M. J. Biercuk, M. C. Llaguno, M. Radosavljevic, J. K. Hyun, A. T. Johnson, and J. E. Fischer, *Appl. Phys. Lett.* **80**, 2767 (2002).
- ²C. Wei, *Appl. Phys. Lett.* **88**, 093108 (2006).
- ³J. Che, T. Cagin, and William A. Goddard III, *Nanotechnology* **11**, 65 (2000).
- ⁴J. Hone, M. C. Llaguno, M. J. Biercuk, A. T. Johnson, B. Batlogg, Z. Benes, and J. E. Fischer, *Appl. Phys. A* **74**, 339 (2002).
- ⁵C. Q. Sun, H. L. Bai, B. K. Tai, S. Li, and E. Y. Jiang, *J. Phys. Chem. B* **107**, 7544 (2003).
- ⁶Y. Kwon, S. Berber, and D. Tomaneck, *Phys. Rev. Lett.* **92**, 015901 (2004).
- ⁷G. Cao, X. Chen, and G. W. Kysar, *J. Mech. Phys. Solids* **54**, 1206 (2006).
- ⁸C. Wei, K. Cho, and D. Srivastava, *Phys. Rev. B* **67**, 115407 (2003).
- ⁹T. Dumitrica, M. Hua, and B. I. Yakobson, *Proc. Natl. Acad. Sci. U.S.A.* **103**, 6105 (2006).
- ¹⁰C. L. Zhang and H. S. Shen, *Appl. Phys. Lett.* **89**, 081904 (2006).
- ¹¹J. Y. Hsieh, J. M. Lu, M. Y. Huang, and C. C. Hwang, *Nanotechnology* **17**, 3920 (2006).
- ¹²T. T. Liu and X. Wang, *Phys. Lett. A* **365**, 144 (2007).
- ¹³X. Chen, X. Wang, and B. Y. Liu, *J. Reinf. Plast. Compos.* **28**, 551 (2009).
- ¹⁴T. Chang and H. Gao, *J. Mech. Phys. Solids* **51**, 1059 (2003).
- ¹⁵L. Shen and J. Li, *Phys. Rev. B* **69**, 045414 (2004).
- ¹⁶A. K. Rappe, C. J. Casewit, K. S. Colwell, W. A. Goddard, and W. M. Ski, *J. Am. Chem. Soc.* **114**, 10024 (1992).
- ¹⁷J. W. Jiang, J. S. Wang, and B. Li, *Phys. Rev. B* **80**, 205429 (2009).
- ¹⁸F. Scarpa, S. Adhikari, and A. S. Phani, *Nanotechnology* **20**, 065709 (2009).
- ¹⁹F. Scarpa and S. Adhikari, *J. Phys. D: Appl. Phys.* **41**, 085306 (2008).
- ²⁰L. J. Gibson and M. F. Ashby, *Cellular Solids: Structure and Properties*, 2nd ed. (Cambridge Press, Cambridge, 1997).
- ²¹Z. C. Tu and Z. O. Yang, *J. Comput. Theor. Nanosci.* **5**, 422 (2008).
- ²²R. C. Batra and A. Sears, *Modell. Simul. Mater. Sci. Eng.* **15**, 835 (2007).
- ²³P. P. Gillis, *Carbon* **22**, 387 (1984).
- ²⁴I. G. Masters and K. E. Evans, *Comput. Struct.* **35**, 403 (1996).
- ²⁵E. Cadelano, P. L. Palla, S. Giordano, and L. Colombo, *Phys. Rev. Lett.* **102**, 235502 (2009).
- ²⁶See supplementary material at <http://dx.doi.org/10.1063/1.3499748> for a detailed description of the model.
- ²⁷L. Wang, Q. Zheng, J. Z. Liu, and Q. Jiang, *Phys. Rev. Lett.* **95**, 105501 (2005).